

CONTINUOUS MEASUREMENT OF IMPULSE RESPONSES ON A CIRCLE USING A UNIFORMLY MOVING MICROPHONE

Nara Hahn and Sascha Spors

Institute of Communications Engineering,
University of Rostock

{nara.hahn, sascha.spors}@uni-rostock.de

ABSTRACT

We propose a continuous measurement technique which can be used to capture a large number of impulse responses within short time. The response of an acoustic system is continuously captured by a moving microphone, and the instantaneous impulse responses are computed by post-processing. The time-variance due to the movement of the microphone is compensated by employing a recently proposed system identification method. In this method, each sample of the captured signal is interpreted as the orthogonal expansion coefficient of the instantaneous impulse response. The impulse responses are computed from the interpolated orthogonal coefficients. This method is applied to the measurement on a circle. Based on the modal bandwidth of the spatio-temporal impulse response, the relation among the length of the impulse response, the angular speed of the microphone, and the effective number of measurements is revealed. The presented measurement technique was used to measure a large number of room impulse responses, and the results were compared with a conventional sequential measurement technique.

Index Terms— Continuous measurement, circular array, sound field analysis, time-variant system identification

1. INTRODUCTION

In sound field analysis, a sound field or a spatio-temporal impulse response is commonly captured at multiple positions, and the desired information is extracted from these [1, 2]. Most frequently, the captured sound field is decomposed into directional components, e.g., by a plane wave decomposition. Such an encoding is advantageous as it is compatible with many sound reproduction techniques, like sound field synthesis or binaural synthesis. In sound field synthesis, each plane wave component is filtered by the corresponding plane wave driving functions, and in binaural synthesis, by the corresponding far-field head-related impulse responses [3, 4].

The spatial resolution of sound field analysis is mainly determined by the number of measurements. The measurement points have to be distributed sufficiently dense, such that the spacing of adjacent points is shorter than half the wavelength of the highest temporal frequency component [5]. The required number of measurements commonly ranges from a few hundreds to several thousands. Performing such a huge amount of measurements is a challenge in sound field analysis. Two conventional strategies are usually used. (1) Simultaneous measurement using a microphone array. Although this is very time-efficient, the original sound field is disturbed by the array itself which is not acoustically transparent. Synchronously capturing such a large number of audio signals is also limited by currently available hardware. Calibration and accurate placement of individual mi-

crophones is also not a trivial task [1, 6]. (2) Sequential measurement using a single or few microphone(s). This circumvents most of above-mentioned problems, at the cost of a long measurement time. As the measurement time increases, the time-variance of the system cannot be ignored, which is often caused by temperature drift in the room or voice coil heating of the loudspeaker. Such system changes are known to limit the signal-to-noise ratio improvement by averaging [7, 8], and also degrade the performance of modal analysis [9].

Alternatively, the impulse responses can be measured continuously by using a single microphone moving on a predefined trajectory. In a continuous measurement, the system of interest is excited, not necessarily but commonly, by a periodic signal, and the response is captured by a continuously moving microphone. The instantaneous impulse responses are computed from the captured signal. Due to its remarkable time-efficiency, continuous measurement techniques may be preferred in high-resolution sound field analysis, where a massive number of impulse responses are needed. A series of continuous measurement techniques have been proposed in the past decade [10–14]. The main differences among the proposed methods are the choice of the excitation signal, the underlying system model, and the compensation of the time-variance due to the movement of the microphone. The methods in [11] and [12] were employed for room impulse responses, while the others were used for head-related impulse responses or binaural room impulse responses [10, 13–15].

In this paper, the method proposed by the authors [14] is used to measure the room impulse responses on a circle using a uniformly moving microphone. It is shown that the effective number of measurements is determined by the angular speed of the microphone and the period of the excitation signal. To avoid temporal aliasing, the latter has to be longer than the impulse response. The maximum allowable angular speed is derived for a given configuration and required spatial resolution. In the following section, the spatial sampling of the impulse responses on a circle is reviewed. Section 3 introduces the employed system identification method, and applies it to circular measurements. In Sec. 4, the measurement results are presented and compared with sequential measurements.

Nomenclature We consider discrete-time signals $s(n)$ with a sampling rate of f_s . The discrete index n and k is used for time-domain signals and impulse responses $h(k)$, respectively. For convenience, the discrete-time Fourier transform is denoted by $S(\omega)$, rather than by $S(e^{i\Omega})$, where $\omega = \Omega f_s$. The angular frequency is related to the temporal frequency by $\omega = 2\pi f$, and its maximum is given by the Nyquist frequency $\omega_{\max} = \pi f_s$. The speed of sound is denoted by c , and the imaginary unit is defined by $i^2 = -1$. Only the horizontal plane ($z = 0$) is considered, and a polar coordinate representation is used, $\mathbf{x} = (r, \phi)$, where $r = \sqrt{x^2 + y^2}$, and $\phi = \tan^{-1}(\frac{y}{x})$.

2. SPATIAL SAMPLING OF A SPATIO-TEMPORAL IMPULSE RESPONSES ON A CIRCLE

The acoustic transmission from a sound source at $\mathbf{x}_s = (r_s, \phi_s)$ to a receiving point $\mathbf{x} = (r, \phi)$ is characterized by the spatio-temporal impulse response $h(\mathbf{x}, \mathbf{x}_s, k)$, or equivalently by the spatio-temporal transfer function $H(\mathbf{x}, \mathbf{x}_s, \omega)$. Throughout this paper, the sound fields are assumed to be produced by a static sound source, and thus, the source position vector \mathbf{x}_s is omitted. For convenience, the term *spatio-temporal* is also omitted, in the remainder.

Consider the transfer function on a circle with radius $r_0 \neq r_s$, centered at the origin. Due to the 2π -periodicity along the polar angle ϕ , it can be represented by the circular harmonics expansion,

$$H(r_0, \phi, \omega) = \sum_{\nu=-\infty}^{\infty} \hat{H}_{\nu}(r_0, \omega) e^{i\nu\phi}, \quad (1)$$

where $e^{i\nu\phi}$ is the ν -th circular harmonic (mode), and $\hat{H}_{\nu}(r_0, \omega)$ the corresponding expansion coefficient (modal strength) given as

$$\hat{H}_{\nu}(r_0, \omega) = \frac{1}{2\pi} \int_0^{2\pi} H(r_0, \phi, \omega) e^{-i\nu\phi} d\phi. \quad (2)$$

If a bounded circular region $r < r_0$ is free of source and scatterer, the modal spectrum $\hat{H}_{\nu}(r, \omega)$ has a low-pass characteristic in the modal domain [1, 2]. While most of the modal energy is concentrated in $|\nu| < \frac{\omega}{c} r_0$, it rapidly decreases as $|\nu|$ increases beyond $\frac{\omega}{c} r_0$. Thus, $\frac{\omega}{c} r_0$ is often considered as the approximate modal bandwidth for a given frequency.

In practice, the transfer function is measured at a finite number of positions. Typically, $H(r_0, \phi, \omega)$ is spatially sampled at equiangular positions, $\phi_m = \frac{2\pi}{M}m$, $m = 0, \dots, M-1$, which can be modeled as multiplication with an impulse train [5], $\sum_{m=0}^{M-1} \frac{M}{2\pi} \delta(\phi - \frac{2\pi m}{M})$, where $\delta(\cdot)$ is the Dirac delta function. In the modal domain, this corresponds to the convolution with an impulse train with period M . This results in spectral replications that appear at inter multiples of M ,

$$\hat{H}'_{\nu}(r, \omega) = \sum_{\mu \in \mathbb{Z}} \hat{H}_{\nu+\mu M}(r, \omega), \quad (3)$$

where $\hat{H}'_{\nu}(r, \omega)$ denotes the modal coefficient of the discretized transfer function. The replicated spectra ($\mu \neq 0$) are superimposed with the original modal spectrum ($\mu = 0$), and thus, modal aliasing occurs.

We are interested in the minimum value of M that avoids modal aliasing in the high-energy part of the modal spectrum ($|\nu| < \frac{\omega}{c} r_0$), such that the aliased energy is kept sufficiently low. As the modal bandwidth is proportional to the temporal frequency ω , the modal bandwidth of a sound field is determined by its maximum temporal frequency ω_{\max} . Considering that the first spectral replications appear at $\nu = \pm M$, the following condition can be derived,

$$M \geq \frac{2\omega_{\max} r_0}{c}. \quad (4)$$

This is often considered as the rule of thumb in modal analysis using circular arrays [2, Eq. (3.43)] [16, Eq. (17)].

3. SYSTEM IDENTIFICATION

In this section, a system identification method is reviewed that is suited for linear time-varying systems [14]. We assume that the sound field captured by the microphone is represented by a linear time-varying finite impulse response (FIR) model,

$$p(n) = \sum_{k=0}^{N-1} s(n-k)h(k, n), \quad (5)$$

where $p(n)$ is the captured (output) signal, $s(n)$ the source (input) signal, and $h(k, n)$ the k -th coefficient of the impulse response at time n . The length of $h(k, n)$ satisfies $N > T_{\max} f_s$, where T_{\max} is the maximum impulse response length, in seconds. In the employed method, the system is periodically excited by a so-called perfect sequence, $\psi(n) = \psi(n+N)$, which satisfies the ideal periodic autocorrelation property,

$$\rho_{\psi\psi}(m) = \sum_{n=0}^{N-1} \psi(n)\psi(n+m) = E \times \delta_{(m \bmod N)0} \quad (6)$$

where δ_{mn} denotes the Kronecker delta, and E is the energy per period. Without loss of generality, E is set to unity.

Equation (6) states that a circularly shifted sequence $\psi(n-m)$ is orthogonal to the original sequence $\psi(n)$, whenever m is not an integer multiple of N . We define a set of functions which consists of N time-reversed and time-shifted perfect sequences,

$$\left\{ \psi(-n), \psi(1-n), \dots, \psi(N-1-n) \right\}. \quad (7)$$

Due to the property (6), it forms an orthonormal basis set for \mathbb{R}^N . By using the basis functions, an impulse response can be represented as,

$$h(k, n) = \sum_{m=0}^{N-1} a_m(n) \psi(-k+m), \quad k = 0, \dots, N-1, \quad (8)$$

where $a_m(n)$ is the time-dependent expansion coefficient. If the system is excited by a perfect sequence $s(n) = \psi(n)$,

$$p(n) = \sum_{k=0}^{N-1} \psi(n-k) \sum_{m=0}^{N-1} a_m(n) \psi(-k+m) \quad (9)$$

$$= \sum_{m=0}^{N-1} a_m(n) \underbrace{\sum_{k=0}^{N-1} \psi(n-k) \psi(m-k)}_{=\delta_{m(n \bmod N)}} \quad (10)$$

$$= a_{(n \bmod N)}(n), \quad (11)$$

which means that the output of the system is the $(n \bmod N)$ -th orthogonal expansion coefficient at time n [14, 17]. In other words, the individual orthogonal components of the system are sequentially excited, and the corresponding coefficients are captured by the microphone. As each $a_m(n)$ is observed only once per period (N samples), it is decimated by a factor of N ,

$$a'_m(n) = \begin{cases} a_m(n) & , \text{if } n \bmod N = m \\ 0 & , \text{else} \end{cases}, \quad (12)$$

where $a'_m(n)$ denotes the decimated coefficients.

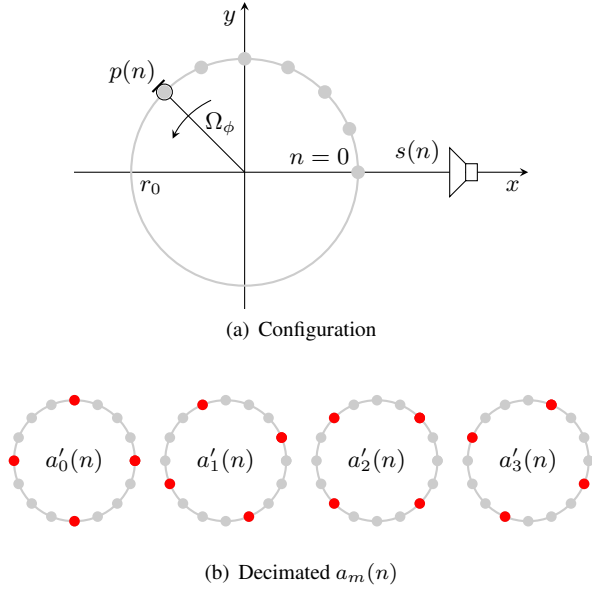


Fig. 1. Continuous measurement on a circle ($N = 4$, $L = 16$). The sound field is produced by a loudspeaker on the x -axis driven by the source signal $s(n)$. A microphone is moving on the circle at an angular speed of Ω_ϕ . The gray circles indicate the position where the discrete-time signals are captured. As shown in (b), the individual expansion coefficients are observed one time per N samples. The red circles indicate the positions where the coefficients are captured. In this example, the effective number of spatial sampling positions is $\frac{L}{N} = 4$.

Now we consider that the microphone is moving on a circle $r = r_0$ at a constant angular speed of $\Omega_\phi > 0$, starting from $\phi_0 = 0$, as shown in Fig. 1(a). The position of the microphone on the circle is $\phi_n = \frac{\Omega_\phi}{f_s} n$, and thus, $h(n, k) = h(\phi_n, k)$ and $a_m(n) = a_m(\phi_n)$. The length of the captured signal within 2π -rotation is $L = 2\pi f_s / \Omega_\phi$ samples. According to (12), each orthogonal coefficient is observed at $\frac{L}{N}$ equiangular points on the circle, as illustrated in Fig. 1(b). The effective number of spatial sampling points is $M_{\text{eff}} = \frac{L}{N} = \frac{2\pi f_s}{\Omega_\phi N}$, and their positions are angularly shifted. The impulse responses cannot be directly computed by (8), as the expansion coefficients belong to different impulse responses. The intermediate values have to be interpolated from the decimated coefficients. Note that, $a_m(n)$ also satisfies the physical properties discussed in Sec. 2. Therefore, to recover $a_m(n)$ accurately, M_{eff} has to fulfill the condition given in (4),

$$M_{\text{eff}} \geq \frac{2\omega_{\text{max}} r_0}{c}. \quad (13)$$

When we substitute $M_{\text{eff}} = \frac{2\pi f_s}{\Omega_\phi N}$ and $\omega_{\text{max}} = \pi f_s$ into (13), the condition for the angular speed is obtained,

$$\Omega_\phi \leq \frac{c}{r_0 N} < \frac{c}{r_0 T_{\text{max}} f_s}, \quad (14)$$

where $N > T_{\text{max}} f_s$ is used in the second inequality. Interestingly, this is very similar to the maximum allowable angular speed derived in [12, Eq. (29)], $\frac{c}{r_0 (T_{\text{max}} f_s - 1)}$, although the approach for continuous measurement is quite different. When (14) is formulated with

respect to the tangential speed of the microphone $v_t = r_0 \Omega_\phi$,

$$\frac{v_t}{c} \leq \frac{1}{N}, \quad (15)$$

meaning that the Mach number should be less than or equal to $\frac{1}{N}$.

If the condition in (13) or (14) is fulfilled, the expansion coefficients can be computed by interpolation filters $g_m(\phi_n)$,

$$\hat{a}_m(\phi_n) = \sum_{l=0}^{M-1} a'_m(\phi_{m+lN}) g_m(\phi_n - \phi_{m+lN}), \quad (16)$$

and finally, the impulse response coefficients are computed from (16) using (8). The employed system identification method is flexible in terms of the types of interpolation filter. In [15], we observed that even a low-order interpolation method, like linear interpolation, gives plausible results when applied to binaural room impulse responses measurement in dynamic acoustic scenes.

4. MEASUREMENT RESULTS AND DISCUSSION

The presented method was used to measure the impulse responses in a rectangular room ($W \times L \times H = 5.8 \text{ m} \times 5.0 \text{ m} \times 3.0 \text{ m}$) at the Institute of Communications Engineering, University Rostock. The room is moderately damped with absorptive material. The measurement setup is similar to Fig. 1(a). The loudspeaker and the measurement circle were placed at the same horizontal plane, at a height of 1.62 m. The radius of the circle was $r_0 = 0.5 \text{ m}$. An omni-directional microphone was mounted on a motorized arm [18]. The sampling frequency of the reproduced and recorded signals was $f_s = 44.1 \text{ kHz}$. The system was excited by a periodic sweep [19], which satisfies (6). The period was 2 s (88200 samples), sufficiently longer than the impulse response of the room. The approximate maximum modal order of the impulse response was 202 for $c = 343 \text{ m/s}$. According to (4), the required number of measurements was 404, and the corresponding angular speed was $0.45^\circ/\text{s}$. We chose $\Omega_\phi = 0.25^\circ/\text{s}$ instead, and thus, the effective number of measurement was $M_{\text{eff}} = 720$. The orthonormal expansion coefficients were interpolated by using a sinc function, symmetrically truncated to a length of 7. For comparison, the same number of impulse responses were sequentially measured using a logarithmic sweep with a length of 2^{17} samples ($\approx 3 \text{ s}$). The measurement time was 26 minutes for the continuous measurement, and about three times longer for the sequential measurement.

In Fig. 3, the impulse responses are shown both for continuous and sequential measurements. In Fig. 3(c) and 3(d), only the earlier parts (0–22 ms) are plotted, where most of the energy is concentrated and the temporal fine structure has perceptual importance. No significant difference can be observed in the temporal structure of the impulse responses. The reflections appearing just after the direct sound ($\approx 7 \text{ ms}$) are caused by the motorized arm that is positioned at the center of the measurement circle. The later parts (145–167 ms) are shown in Fig. 3(a) and 3(b). Note that the levels have different scale than Fig. 3(c) and 3(d). The continuously measured impulse responses suffer from slight artifacts, that seems to be caused by vibration of the motor and frictional noise of the cables.

To evaluate the similarities and difference of the two data sets, the cross-correlation $\rho(\phi, \tau)$ was considered rather than the mean square difference, as the latter is too sensitive to time shifts. In fact, the impulse responses measured in the same setup do not differ significantly in its waveforms, but may have time offsets due

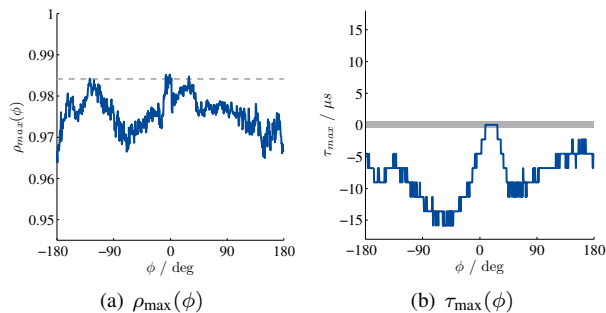


Fig. 2. Comparison of the continuous measurements and the sequential measurements. (a) The maximum value of the normalized cross-correlation, and (b) the corresponding time lag.

to the variability of the speed of sound. Prior to the computation of the cross-correlation, the impulse responses were upsampled by a factor of 10. The cross-correlation was normalized by the root mean squares of both impulse responses. The maximum value of $\rho(\phi, \tau)$ was considered as a similarity measure of the waveforms. The time-lag giving the maximum cross-correlation was computed, $\tau_{\max} = \arg \max_{\tau} \{\rho(\phi, \tau)\}$, which is an estimate of the time delay difference of the two impulse responses. For two perfectly identical impulse responses, the maximum value of the normalized cross-correlation would be equal to 1 appearing at $\tau = 0$. In Fig. 2, the results are indicated by dark blue lines. In 2(a), the maximum correlation is mostly in the range between 0.97 and 0.98. The value of τ_{\max} is quantized with an interval of $\frac{1}{10f_s} \approx 2.268 \mu\text{s}$. It has only non-positive values, meaning that the continuous measurements tend to be delayed with respect to the sequential measurements. The maximum difference is about $15 \mu\text{s}$, corresponding to about 0.7 samples in the original sampling rate $f_s = 44.1 \text{ kHz}$. As a reference, the cross-correlation and the time delay were also computed for impulse responses measured 720 times at a fixed position. Among them, 720 combinations were randomly selected and the cross-correlations were computed. The mean value of the maximum cross-correlation (0.984) is shown with a gray dashed line in Fig. 2(a), whereas the range corresponding to the standard deviation of the time delay ($\pm 0.528 \mu\text{s}$) is shown with a shaded region in Fig. 2(b). It can be concluded that the waveforms of the impulse responses are in a good accordance with each other, whereas there exists a slight time shift which is less than 1 sampling period. It has to be noted that the continuous and sequential measurements have not been taken at the same time. This might have caused some of the differences.

To observe the perceptual properties, both measurements were used to generate a number of listening examples. Speech, castanets, and wide-band pink noise were filtered with the individual impulse responses. In informal listening, no difference can be perceived. The listening examples are available for download at http://spatialaudio.net/continuous_measurement/.

It is worth mentioning some practical issues in continuous measurement. (1) As the microphone has to be accelerated until it reaches the target angular speed, it has to be rotated slightly more than 2π rad. The accelerating and decelerating parts of the captured signal are discarded. (2) In our measurement setup, the motion of the motor and excitation signal were not perfectly synchronized. To tackle this problem, an additional microphone was placed at a fixed position, $(r_0, 0)$. The captured signal of that static microphone was later used to estimate the time instant when the moving microphone was

at $\phi = 0$. (3) The captured signal is often contaminated by vibration and mechanical noise caused by the motorized arm, which strongly depends on the rotational speed of the motor. In some cases, the maximum angular speed derived in this paper might be impractical, due to the resulting poor signal-to-noise ratio. Though, it is still an open question how much noise is allowed in impulse response measurements, e.g., for virtual acoustics applications.

5. CONCLUSION

We proposed a new continuous measurement technique for room impulse responses. A massive number of impulse responses can be measured within a short time frame. The maximum angular speed of the microphone was derived based on the modal bandwidth of the sound field on a circle. The presented method was used to continuously measure a set of impulse responses, and the results were compared with conventional sequential measurements. While the proposed method is much more time-efficient, the measurement results were comparable. The proposed technique has to be further verified by using the measured impulse responses in sound field synthesis or binaural synthesis [3, 4].

REFERENCES

- [1] Achim Kuntz, *Wave Field Analysis Using Virtual Circular Microphone Arrays*, Verlag Dr. Hut, 2008.
- [2] Heinz Teutsch, *Modal Array Signal Processing: Principles and Applications of Acoustic Wavefield Decomposition*, vol. 348, Springer Science & Business Media, 2007.
- [3] Edo Hulsebos, Diemer de Vries, and Emmanuelle Bourdillat, "Improved microphone array configurations for auralization of sound fields by wave-field synthesis," *Journal of the Audio Engineering Society*, vol. 50, no. 10, pp. 779–790, 2002.
- [4] Sascha Spors, Hagen Wierstorf, and Matthias Geier, "Comparison of modal versus delay-and-sum beamforming in the context of data-based binaural synthesis," in *Audio Engineering Society Convention 132*, 2012.
- [5] Bernd Girod, Alexander Stenger, and Rudolf Rabenstein, *Signals and Systems*, Wiley, 2001.
- [6] Boaz Rafaely, "Analysis and design of spherical microphone arrays," *Speech and Audio Processing, IEEE Transactions on*, vol. 13, no. 1, pp. 135–143, 2005.
- [7] Michael Vorländer and Malte Kob, "Practical aspects of MLS measurements in building acoustics," *Applied Acoustics*, vol. 52, no. 3, pp. 239–258, 1997.
- [8] Peter Svensson and Johan L. Nielsen, "Errors in MLS measurements caused by time variance in acoustic systems," *Journal of the Audio Engineering Society*, vol. 47, no. 11, pp. 907–927, 1999.
- [9] Benjamin Bernschütz, Christoph Pörschmann, Sascha Spors, and Stefan Weinzierl, "Zeitinvarianzen durch Temperaturveränderung bei sequentiellen sphärischen Mikrofonarrays im Plane Wave Decomposition Verfahren," in *German Annual Conference on Acoustics (DAGA)*, Düsseldorf, Germany, Mar. 2011.
- [10] Christiane Antweiler, Aulis Telle, Peter Vary, and GeraldENZner, "Perfect-sweep NLMS for time-variant acoustic system identification," in *Acoustics, Speech and Signal Processing (ICASSP), 2012 IEEE International Conference on*, 2012, pp. 517–520, IEEE.
- [11] Edo Maria Hulsebos, *Auralization using Wave Field Synthesis*, Ph.D. thesis, TU Delft, Delft University of Technology, 2004.
- [12] Thibaut Ajdler, Luciano Sbaiz, and Martin Vetterli, "Dynamic measurement of room impulse responses using a moving microphone," *The Journal of the Acoustical Society of America*, vol. 122, no. 3, pp. 1636–1645, 2007.

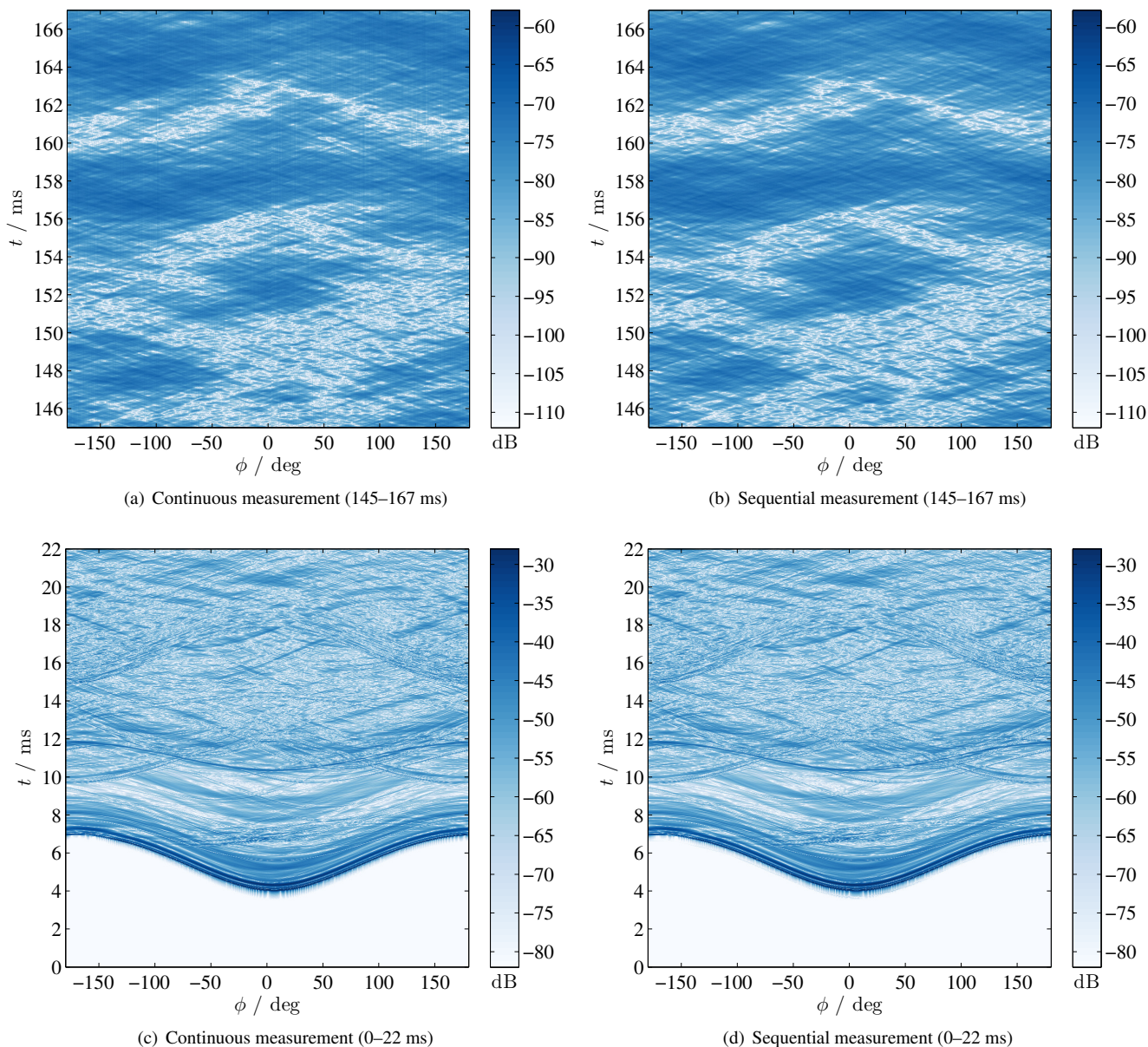


Fig. 3. Room impulse responses, $20 \log_{10} |h(r_0, \phi, k)|$. Each vertical slice shows the impulse response at the corresponding angle.

- [13] Kimitoshi Fukudome, Toshimitsu Suetsugu, Takuya Ueshin, Ryo Idegami, and Kazuki Takeya, “The fast measurement of head related impulse responses for all azimuthal directions using the continuous measurement method with a servo-swiveled chair,” *Applied Acoustics*, vol. 68, no. 8, pp. 864–884, 2007.
- [14] Nara Hahn and Sascha Spors, “Identification of dynamic acoustic systems by orthogonal expansion of time-variant impulse responses,” in *Communications, Control and Signal Processing (ISCCSP), 2014 6th International Symposium on*, 2014, pp. 161–164, IEEE.
- [15] Nara. Hahn and Sascha. Spors, “Measurement of time-variant binaural room impulse responses for data-based synthesis of dynamic auditory scenes,” in *German Annual Conference on Acoustics (DAGA)*, Oldenburg, Germany, Mar. 2014.
- [16] Darren B. Ward and Thushara D. Abhayapala, “Reproduction of a plane-wave sound field using an array of loudspeakers,” *Speech and Audio Processing, IEEE Transactions on*, vol. 9, no. 6, pp. 697–707, 2001.
- [17] Alberto Carini, “Efficient NLMS and RLS algorithms for perfect periodic sequences,” in *Acoustics Speech and Signal Processing (ICASSP), 2010 IEEE International Conference on*, 2010, pp. 3746–3749, IEEE.
- [18] Benjamin Bernschütz, Christoph Pörschmann, Sascha Spors, and Stefan Weinzierl, “Entwurf und Aufbau eines variablen sphärischen Mikrofonarrays für Forschungsanwendungen in Raumakustik und virtual Audio,” in *German Annual Conference on Acoustics (DAGA)*, Berlin, Germany, Mar. 2010.
- [19] Yōiti Suzuki, Futoshi Asano, Hack-Yoon Kim, and Toshio Sone, “An optimum computer-generated pulse signal suitable for the measurement of very long impulse responses,” *The Journal of the Acoustical Society of America*, vol. 97, no. 2, pp. 1119–1123, 1995.